Available online at www.sciencedirect.com
ScienceDirect
Acta Materialia 56 (2008) 925–933
Acta MATERIALIA
www.elsevier.com/locate/actamat

Wetting transition of grain-boundary triple junctions

B.B. Straumal [a,b,*], O. Kogtenkova [b], P. Zięba [c]

[a] Max-Planck-Institut für Metallforschung, Heisenbergstrasse 3, 70569 Stuttgart, Germany
[b] Institute of Solid State Physics, Russian Academy of Sciences, Chernogolovka, Moscow District 142432, Russia
[c] Institute of Metallurgy and Materials Science, Polish Academy of Sciences, Reymonta Street 25, 30-059 Cracow, Poland

Received 12 August 2007; received in revised form 7 October 2007; accepted 9 October 2007
Available online 11 January 2008

Abstract

The wetting phase transition of grain boundaries (GBs) and grain-boundary triple junctions (GB TJs) by the melt has been studied in the Al–30 wt.%Zn and Al–10 wt.%Zn–4 wt.%Mg polycrystals. The condition of complete wetting is weaker for TJs ($\sigma_{GB} > \sqrt{3}\sigma_{SL}$) than that for GBs ($\sigma_{GB} > 2\sigma_{SL}$), σ_{GB} being the GB energy and $2\sigma_{SL}$ being the energy of the solid/liquid interphase boundary. As a result the temperature of TJ wetting transition should be lower than that of GB wetting transition T_{wGB}. It has been experimentally observed for the first time that TJs become completely wetted at T_{wTJ}, which is about 10–15 °C below T_{wGB}.

Keywords: Grain boundaries; Triple junctions; Al–Zn–Mg alloys; Wetting phase transition

1. Introduction

The idea that the transition from incomplete to complete surface wetting is a phase transformation was first proposed by J.W. Cahn in 1977 [1]. Later this idea was successfully applied for grain boundaries (GBs) and old data on GB wetting were reconsidered from this point of view [2–5]. GB wetting phase transformation proceeds at the temperature T_{wGB}, where GB energy σ_{GB} becomes equal to the energy $2\sigma_{SL}$ of two solid/liquid interfaces. Above T_{wGB} GB is substituted by a layer of the melt. GB wetting phase transformations are important for liquid phase sintering of metals and ceramics [6,7], semi-solid metal processing [8], thixotropic casting [9], exploitation of heat-exchanger tubes filled with liquid metal [10] etc. GB wetting phase transitions have recently been included in the traditional bulk phase diagrams of several systems [2–5,11–14]. However, semi-solid polycrystals contain not only planar defects like GBs and interphase boundaries but also line defects like GB triple junctions (TJs). In particular, TJs control the grain growth in nanograined materials [15,16]. Nevertheless, TJ wetting remained for a long time "in the shadow" of GB wetting phenomena. Can the temperature of TJ wetting transition T_{wTJ} differ T_{wGB}? Already McLean mentioned that the wetting should occur at TJs under less restrictive conditions than at GBs [17]. Referring to the older work of Smith [18] he showed by means of a very simple calculation that GBs are completely wetted if $\sigma_{GB} > 2\sigma_{SL}$ and TJs are wetted if $\sigma_{GB} > \sqrt{3}\sigma_{SL}$ (here σ_{GB} is the GB energy and σ_{SL} is the energy of solid/liquid interphase boundaries, IBs). This fact logically leads to the difference in the temperatures of the wetting transition for GBs and TJs (see the Section 4 below). There are numerous experimental evidence that TJs can be wetted by a second phase even if GBs remain dry or incompletely wetted. It is very typical, especially for oxides and nitrides, where the "pockets" of the liquid (or amorphous) phase in the TJs are frequently contact with "dry" GBs containing only a thin layer of a liquid-like GB phase. Typical examples can be found in the Y_2O_3-doped AlN [19], La-doped $SrTiO_3$ [20], Bi_2O_3-doped ZnO [21,22], Ca-doped Si_3N_4 [23].

* Corresponding author. Address: Institute of Solid State Physics, Russian Academy of Sciences, Chernogolovka, Moscow District 142432, Russia. Tel.: +7 0956768673; fax: +7 0952382326.
E-mail address: straumal@issp.ac.ru (B.B. Straumal).

1359-6454/$34.00 © 2007 Published by Elsevier Ltd on behalf of Acta Materialia Inc.
doi:10.1016/j.actamat.2007.10.043

Even for the case of magma migration and storage, the partially molten aggregates were considered, where the capillary action on partially wetted GBs tends to retain melt in the tubules along TJs [24]. When the slabs of Al-based alloys are heated up to the constant temperature for the semi-solid forming, all GBs become wetted by the melt after the heating is finished. However, melting started at the TJs during the heating and progressed along GBs [25]. Later evidence can be considered as the best indication existing in the literature that $T_{wTJ} < T_{wGB}$. Nevertheless, to the best of our knowledge until now there was no direct experimental evidence that TJs become completely wetted at the temperature T_{wTJ}, which is different from that of GB wetting phase transition T_{wGB}. We choose for our experiments Al–30 wt.%Zn and Al–10 wt.%Zn–4 wt.%Mg polycrystalline alloys for several reasons. First, the Al–Zn system is a base of high strength Al-alloys of 7xxx series [26]. Second, it is known that GB wetting phase transition takes place in the Al–Zn and Al–Mg systems [27,28]. Third, the high-rate superplasticity occurs in the nanograined 7xxx alloys close to the solidus line [29,30]. The extremely high plasticity of these alloys is most probably driven by the presence of the thin layers of GB liquid-like phase [31].

2. Experimental

Al (99.999 wt.%), Zn (99.999 wt.%) and Mg (99.95 wt.%) were utilized for the preparation of cylinders ($Ø \approx 7$ mm) of Al–30 wt.%Zn and Al–10 wt.%Zn–4 wt.%Mg alloys. For the wetting experiments, slices (2 mm thick) were cut from the ingots and sealed into evacuated silica ampoules with a residual pressure of approximately 4×10^{-4} Pa at room temperature. Then, samples were annealed for three days at temperatures between 490 and 630 °C, in steps of 7–8 °C. The annealing temperature was maintained constant with an accuracy of ±1 °C. After annealing, the specimens were quenched in water. After quenching, for the metallographic analysis the specimens were embedded in resin and then mechanically ground and polished, using 1 μm diamond paste in the last polishing step. The samples were inspected by means of scanning electron microscopy (SEM) and light microscopy (LM). SEM investigations have been carried out in a Tescan Vega TS5130 MM microscope equipped by the LINK energy-dispersive spectrometer produced by Oxford Instruments. Light microscopy has been performed using Neophot-32 light microscope equipped with 10 Mpix Canon Digital Rebel XT camera.

A quantitative analysis of the wetting transition was performed adopting the following criterion: every GB was considered to be completely wetted only when a liquid layer had covered the whole GB (all three GBs in Fig. 1h); if such a layer appeared to be interrupted, the GB was regarded as a partially wetted (all three GBs in Fig. 1b,d,e). If no liquid phase was present in a GB, it was regarded as dry (all three GBs in Fig. 1a). Similarly, a GB triple junction was regarded as wetted if a "star" of liquid phase was present in a TJ (Fig. 1c,d,f,g,h), in other cases it was regarded as dry (Fig. 1a,e). Careful sectioning of annealed samples did not reveal any partially wetted TJs (like in the scheme Fig. 1b). Therefore, they were not taken into account. Along with dry TJs, we counted separately the wetted TJs in contact with three (Fig. 1c), two

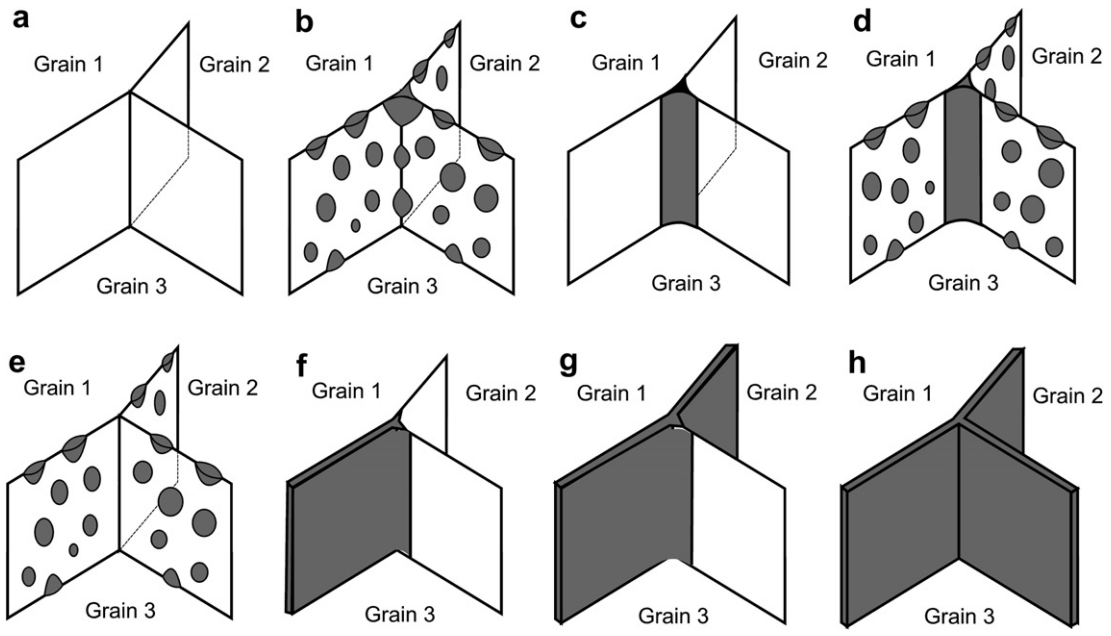

Fig. 1. Grain-boundary (GB) triple joint (TJ) between grains 1, 2, and 3. (a) Dry TJ in contact with dry GBs. (b) Partially wetted TJ in contact with three partially wetted GBs. (c) Completely wetted TJ in contact with three dry GBs. (d) Completely wetted TJ in contact with three partially wetted GBs. (e) Dry TJ in contact with three partially wetted GBs. (f) Completely wetted TJ in contact with one completely wetted GB. (g) Completely wetted TJ in contact with two completely wetted GBs. (h) Completely wetted TJ in the contact with three completely wetted GBs.

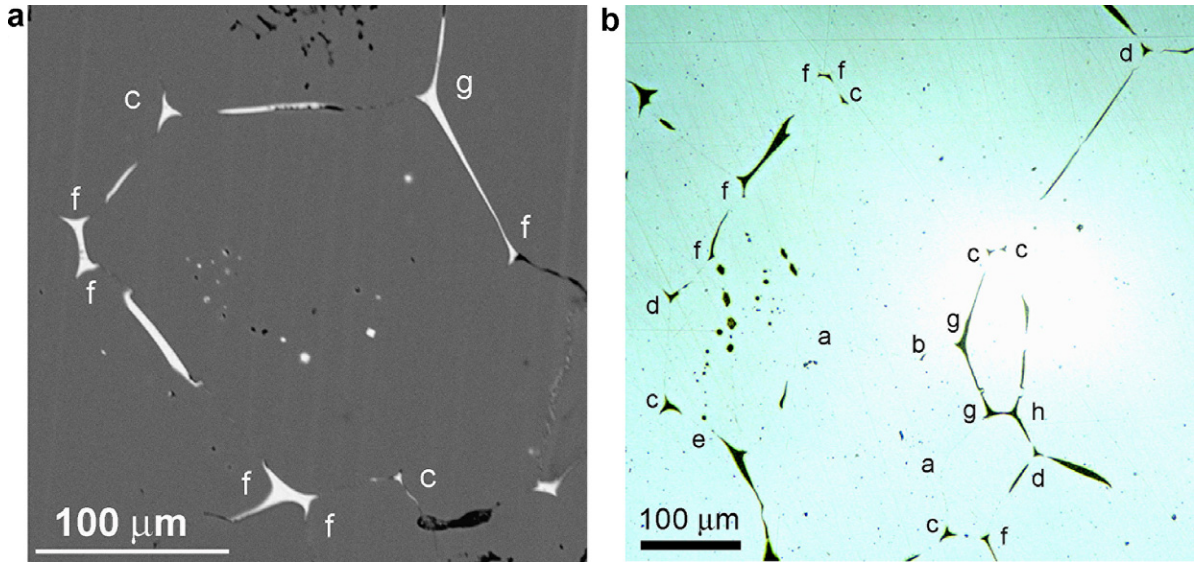

Fig. 2. (a) Microstructure of the Al–10 wt.%Zn–4 wt.%Mg alloy after annealing at 540 °C obtained by SEM (backscattered electrons). Al-rich matrix appears gray; GB and TJ wetting layers appear white. (b) Microstructure of the Al–10 wt.%Zn–4wt.%Mg alloy after annealing at 547 °C obtained by light microscopy. Al-rich matrix appears white; GB and TJ wetting layers appear dark. Variously wetted GBs and TJs are marked by letters according to the scheme in Fig. 1.

(Fig. 1f), one (Fig. 1g), or none (Fig. 1h) dry or partially wetted GBs. At least 1000 GBs and/or TJs were analysed at each temperature. Typical micrographs obtained by SEM and light microscopy are shown in Fig. 2. Different kinds of wetted GBs and TJs are marked in Fig. 2 by letters corresponding to the scheme in Fig. 1.

3. Results

In Fig. 3 part of the Al–Zn bulk phase diagram is shown. Thick solid lines denote bulk phase equilibria [32]. Crosses denote the experimental points in this work. In Fig. 4a the temperature dependencies of the percentage of completely wetted, partially wetted and dry GBs are shown for Al–30 wt.%Zn polycrystals. Below bulk solidus ($T_s = 536$ °C) liquid phase was not present in a system, and only dry GBs existed. Above T_s the percentage of completely dry GBs continuously decreased with increasing temperature and reached zero between 562 and 570 °C. The partially wetted GB appeared in the polycrystal above T_s, their percentage also decreased with increasing temperature. On the opposite, the percentage of completely wetted GBs continuously increased with increasing temperature.

In Fig. 4b the temperature dependencies of the percentage of wetted TJs are shown for Al–30 wt.%Zn polycrystals. They are subdivided into four groups: wetted TJs in contact with three fully wetted GBs (see scheme in Fig. 1c), two fully wetted GBs (Fig. 1f), one fully wetted GBs (Fig. 1g), or three dry or partially wetted GBs (Fig. 1h). Using the careful layer-by-layer polishing we tried to resolve the fully wetted (Fig. 1d) and partially wetted TJs (Fig. 1b) but did not succeed. Therefore, the partially wetted TJs (Fig. 1b) are not represented by a separate group in Fig. 4. Below bulk solidus ($T_s = 536$ °C) liquid phase was not present in a system, and wetted TJs were also absent. Above T_s the wetted TJs appeared. Since the amount of completely wetted GBs was low at 540 °C, no TJs surrounded by three wetted

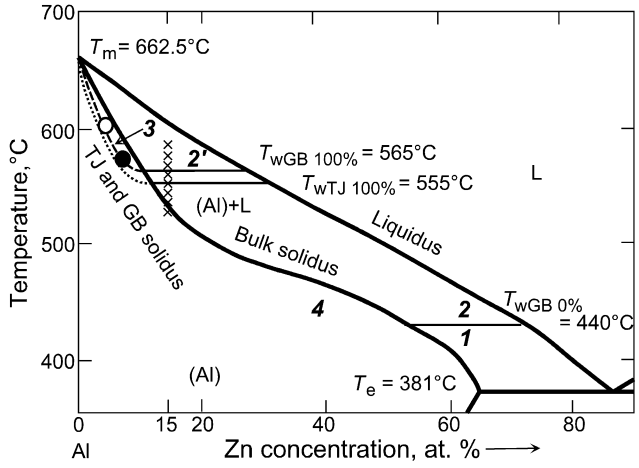

Fig. 3. A part of the Al–Zn phase diagram. Thick solid lines denote bulk phase equilibria [32]. (Al) is the single-phase region where only the Al-based solid solution is in equilibrium in the bulk. L is the single-phase region of a liquid phase (melt). In the (Al) + L two-phase region the Al-based solid solution coexists with the melt. Thin solid lines in the (Al) + L region are the tie-lines of the GB and TJ wetting phase transformation experimentally obtained in this work and in Ref. [27]. They denote the minimal $T_{wGB0\%}$ and maximal $T_{wGB100\%}$ temperatures of GB wetting phase transition, and also maximal $T_{wTJ100\%}$ temperatures of TJ wetting phase transition. The thin dashed line denotes the hypothetic GB solidus line starting from $T_{wGB100\%}$. The thin dotted line denotes the hypothetic TJ solidus line starting from $T_{wTJ100\%}$. Between bulk solidus and GB or TJ solidus GBs or TJs contain a thin equilibrium layer of a liquid-like GB phase [31,37]. Crosses denote the experimental points in this work. Open circle denotes the experimental point where the quenched liquid-like phase was observed in the TJs of the Al–5 at.%Zn alloy [31]. Full circle denotes the temperature where the melting of fine-grained Al–7.5 at.%Zn polycrystal starts [37].

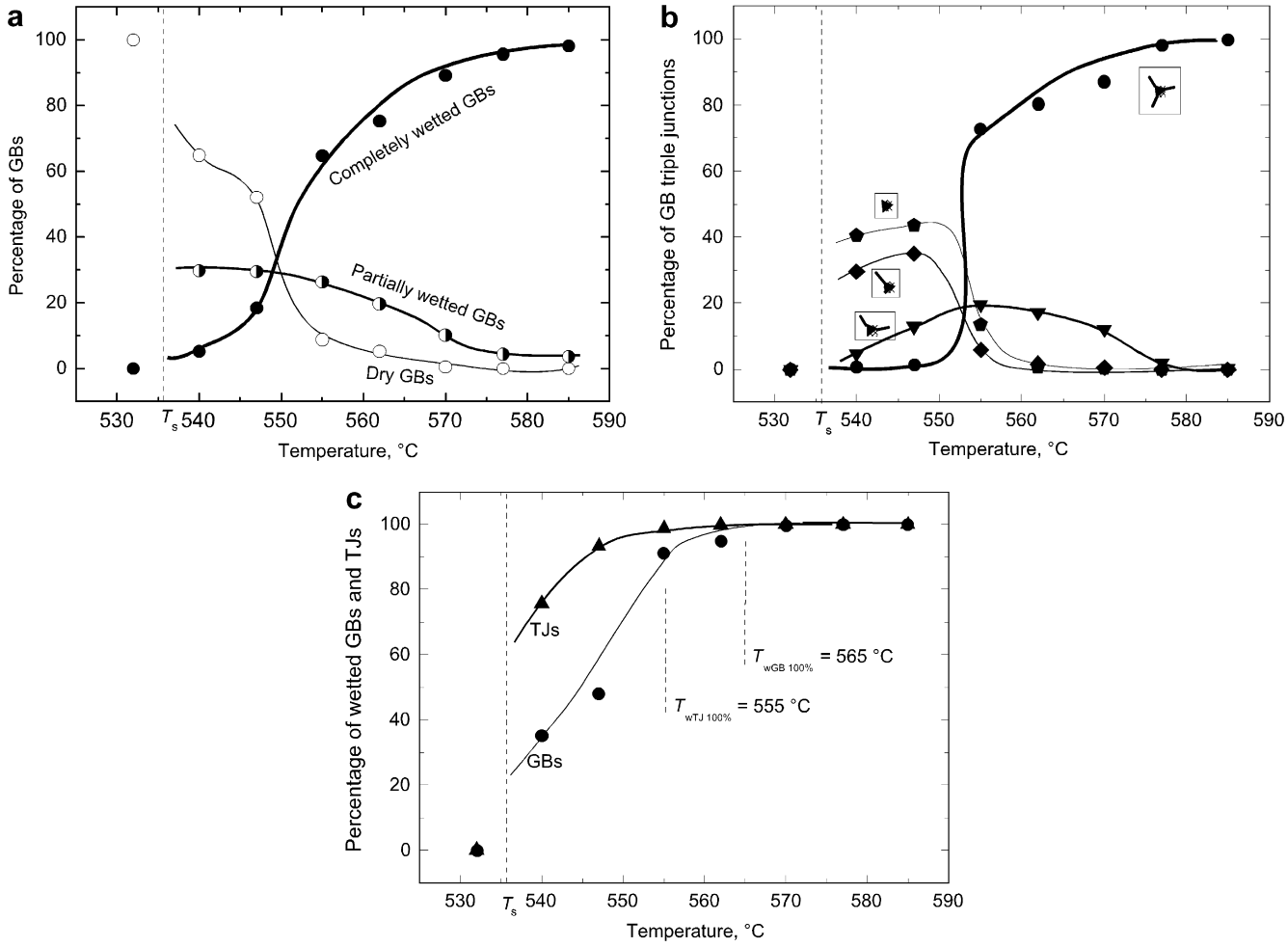

Fig. 4. Al–30 wt.%Zn polycrystals. Temperature dependencies of the percentage of: (a) completely wetted, partially wetted and dry GBs; (b) wetted TJs subdivided into four groups: wetted TJs in the contact with three completely or partially wetted GBs (see scheme in the Fig. 1h), two wetted GBs (Fig. 1g), one wetted GB (Fig. 1f), or three dry GBs (Fig. 1e); (c) total amount of fully and partially wetted GBs and TJs.

GBs were present. The percentage of "standing alone" wetted TJs and TJs in contact with one wetted GB was maximal at 547 °C, by further increase of temperature they disappeared from the polycrystals. In contrast, the percentage of TJs in the contact with two and three wetted GBs increased with increasing temperature. However, the amount of TJs in contact with two wetted GBs reached a maximum of about 20% at 555 °C. At higher temperatures such TJs also disappear from the microstructure, only TJs in contact with three wetted GBs remained.

In Fig. 4c the temperature dependencies of percentage of wetted GBs and TJs are compared. These are the sums of all classes of wetted GBs and TJs respectively (in other words, it is the 100% of all GBs or TJs minus a percentage of dry GBs or TJs). It can be seen that the percentage of wetted TJs is always higher than that of wetted GBs. As a result, the wetting transition for TJs proceeds at the temperature $T_{wTJ100\%} = 555$ °C, which is lower than the wetting transition temperature $T_{wGB100\%} = 565$ °C for GBs.

In Fig. 5 section of the Al–Zn–Mg bulk phase diagram is shown. Thick solid lines denote bulk phase equilibria. The solidus and liquidus lines were obtained in Ref. [5] using the interpolation of solidus and liquidus lines for the binary Al–Zn and Al–Mg phase diagrams from Ref. [24]. Crosses denote the experimental points in this work. In Fig. 6a the temperature dependencies of the percentage of completely wetted, partially wetted and dry GBs are shown for Al–10 wt.%Zn–4 wt.% Mg polycrystals. Below bulk solidus ($T_s = 492$ °C) liquid phase was not present in a system, and only dry GBs existed. Above T_s the percentage of completely dry GBs continuously decreased with increasing temperature and reached zero at 585 °C. The partially wetted GB appeared in the polycrystal above T_s. Their percentage first increased, reached maximum at 540 °C and then decreased with increasing temperature, coming to zero at 585 °C. On the opposite, the percentage of completely wetted GBs continuously increased with increasing temperature.

In Fig. 6b the temperature dependencies of the percentage of wetted TJs are shown for Al–10 wt.%Zn–4 wt.% Mg polycrystals. Similarly to Fig. 4b, they are also subdivided into four groups. Below bulk solidus ($T_s = 492$ °C) liquid

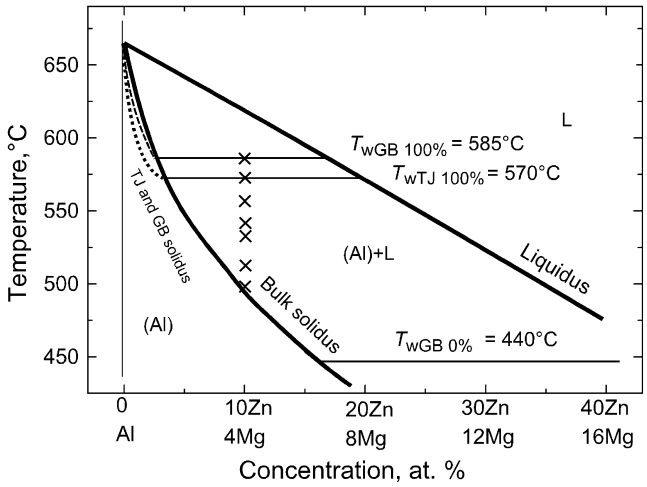

Fig. 5. Section of the Al–Zn–Mg bulk phase diagram. Thick solid lines denote bulk phase equilibria. The solidus and liquidus lines were obtained in Ref. [5] using the interpolation of solidus and liquidus lines for the binary Al–Zn and Al–Mg phase diagrams from Ref. [32]. Thin solid lines in the (Al) + L region are the tie-lines of the GB and TJ wetting phase transformation experimentally obtained in this work. They denote the maximal temperatures of GB $T_{wGB100\%}$ and TJ $T_{wTJ100\%}$ wetting phase transition. Minimal temperature $T_{wGB0\%}$ of GB wetting phase transition was obtained by the extrapolation to 0% (Fig. 6). The thin dashed line denotes the hypothetic GB solidus line starting from $T_{wGB100\%}$. The thin dotted line denotes the hypothetic TJ solidus line starting from $T_{wTJ100\%}$. Between bulk solidus and GB or TJ solidus GBs or TJs contain a thin equilibrium layer of a liquid-like GB phase. Crosses denote the experimental points obtained in this work.

phase was not present in a system, and wetted TJs were also absent. Above T_s the wetted TJs appeared. No TJs surrounded by three wetted GBs were present below 540 °C. The percentage of "standing alone" wetted TJs and TJs in contact with one or two wetted GB was maximal at 557 °C; by further increase of temperature they disappeared from the polycrystals. On the opposite, the percentage of TJs in contact with three wetted GBs increased with increasing temperature, reaching 100% at 585 °C.

In Fig. 6c the temperature dependencies of percentage of wetted GBs and TJs are compared. These are the sums of all classes of wetted GBs and TJs respectively (in other words, it is the 100% of all GBs or TJs minus a percentage of dry GBs or TJs). It can be seen that the percentage of wetted TJs is always higher than that of wetted GBs. As a result, the wetting transition for TJs proceeds at the temperature $T_{wTJ100\%} = 570$ °C, which is lower than the wetting transition temperature $T_{wGB100\%} = 585$ °C for GBs. The minimal temperature for the GB wetting phase transition $T_{wGB0\%} = 480$ °C can be estimated by the extrapolation of the GB line to 0%.

4. Discussion

Consider a grain-boundary in a two-component (or multi-component) alloy being in an equilibrium contact with a melt. Melt can completely wet a GB if $\sigma_{GB} > 2\sigma_{SL}$, i.e. if the GB energy is higher than the energy of two solid/liquid IBs. In case of a full GB wetting the GB (Fig. 7a) has to be substituted by a layer of a liquid phase and two solid/liquid IBs (Fig. 7b). Consider now the GB triple joint in the same alloy. Melt may wet also a triple joint. In this case a trigonal prism filled by a liquid phase substitutes a TJ (Fig. 7c,d). A star of three GBs (Fig. 7c) is substituted by a triangle of solid/liquid IBs (Fig. 7d). In the simplest case of an ideal symmetrical TJ with equal σ_{GB} for all three GBs the wetting condition is $\sigma_{GB} > \sqrt{3}\sigma_{SL}$ [17,18]. It is weaker than similar criteria for GB wetting. We consider here a wetted TJ of macroscopic dimension (at least several microns) and, therefore, neglect in a first approach the energy of TJ σ_{TJ}. Both σ_{GB} and σ_{SL} decrease with increasing temperature due to entropy reasons (Fig. 7e). If temperature dependencies $\sigma_{GB}(T)$ and $2\sigma_{SL}(T)$ intersect at T_{wGB} below a meting (liquidus) temperature T_m, a GB wetting phase transformation takes place at T_{wGB}. Below T_{wGB} a GB can exist in an equilibrium contact with a melt. Above T_{wGB} a GB has to be substituted by a layer of a liquid phase and cannot exist in an equilibrium contact with a melt. The temperature dependence $\sqrt{3}\sigma_{SL}(T)$ lies below the dependence $2\sigma_{SL}(T)$ (Fig. 7e). Therefore, $\sqrt{3}\sigma_{SL}(T)$ intersects with $\sigma_{GB}(T)$ at a temperature T_{wTJ}, which is below T_{wGB}. As a result, the completely wetted GBs are absent in a polycrystal in the temperature interval between T_{wTJ} and T_{wGB}, but completely wetted TJs can exist below T_{wGB} and above T_{wTJ}. This phenomenon was observed in this work in the Al–30 wt.%Zn and Al–10 wt.%Zn–4 wt.%Mg polycrystals. The difference $(T_{wGB} - T_{wTJ}) = 15$ °C for Al–10 wt.%Zn–4 wt.%Mg alloy and for the Al–30 wt.%Zn alloy $(T_{wGB} - T_{wTJ}) = 20$ °C. The penetration kinetics of liquid phase also differs for GBs and TJs. It has been observed in the Al–Sn and Cu–Bi systems that above T_{wGB} the Sn- or Bi-rich melt penetrates along TJs in Al and Cu much deeper than along GBs [33,34]. This means that if the melt penetrates into a polycrystal at the temperature above $T_{wGB100\%}$ and all GBs have to be wetted, the penetration along TJs proceeds with higher rate than along GBs. As a result at a certain distance from the surface, below the front of GB liquid-phase penetration, the tubules filled by a melt were seen in the polycrystals [33,34], similar to those observed in the semi-solid Al-based forgings [25] or in the semi-solid earth magma [24].

In Fig. 8 the semi-quantitative scheme is shown for the temperature dependence of interfacial energies illustrating results obtained in this work. Thick lines correspond to the ternary Al–10 wt.%Zn–4 wt.%Mg alloy, thin lines correspond to the binary Al–30 wt.%Zn alloy. The maximal temperature of the GB wetting phase transition $T_{wGB100\%} = 585$ °C in the ternary alloy corresponds to the intersection of dependencies $2\sigma_{SL}(T)$ and $\sigma_{GBmin}(T)$. The $T_{wTJ} = 570$ °C point for ternary alloys is determined by the intersection of the same dependence $\sigma_{GBmin}(T)$ and $\sqrt{3}\sigma_{SL}(T)$ line, which is positioned about 15%

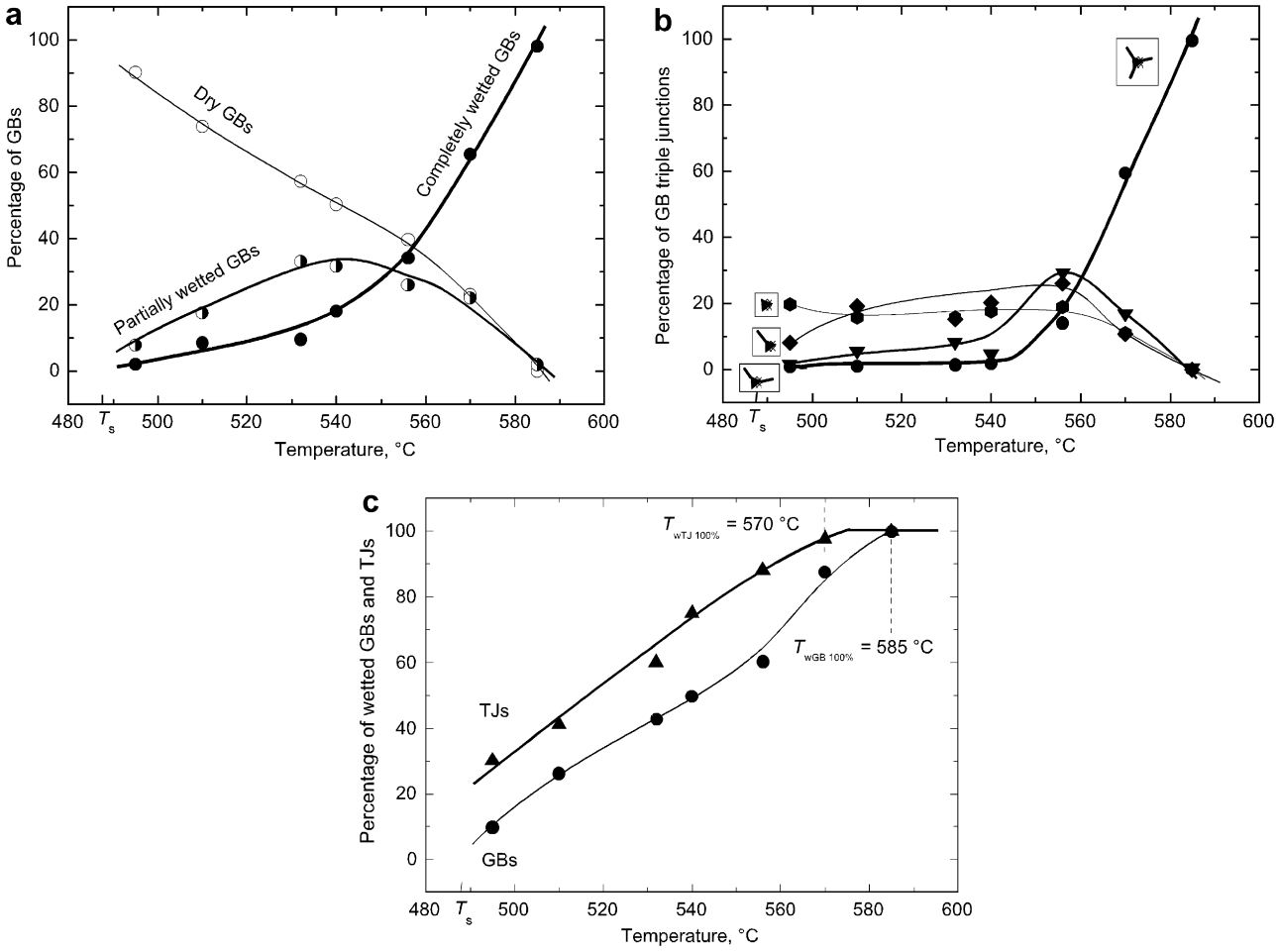

Fig. 6. Al–10 wt.%Zn–4 wt.%Mg polycrystals. Temperature dependencies of the percentage of (a) completely wetted, partially wetted and dry GBs; (b) wetted TJs subdivided into four groups: wetted TJs in the contact with three completely or partially wetted GBs (see scheme in Fig. 1h), two wetted GBs (Fig. 1g), one wetted GB (Fig. 1f), or three dry GBs (Fig. 1e); (c) total amount of fully and partially wetted GBs and TJs.

(i.e. $2-\sqrt{3}$) below the $2\sigma_{SL}(T)$ line. The minimal temperature of the GB wetting phase transformation $T_{wGB0\%} = 480$ °C for the ternary alloy corresponds to the intersection of $2\sigma_{SL}(T)$ and $\sigma_{GBmax}(T)$ dependencies. The value $T_{wGB0\%} = 480$ °C is determined by the extrapolation of data presented in Fig. 6 to the zero percentage of the wetted GBs. σ_{GBmax} in this scheme is supposed to be about two times higher than σ_{Gbmin}; this is a realistic estimation for the most metallic alloys [5,35]. Thin lines represent a similar scheme for $T_{wGB100\%}$ and T_{wTJ} for the binary Al–30 wt.%Zn alloy. If we suppose that $\sigma_{GBmin}(T)$ has the same slope both in ternary and binary alloys, the slope of curve has to be higher in the binary Al–30 wt.%Zn alloy in comparison with ternary Al–10 wt.%Zn–4 wt.%Mg alloy. Only in this case we would obtain the lower difference between $T_{wGB100\%}$ and T_{wTJ} for the binary alloy in comparison with a ternary one since the ratio $2{:}\sqrt{3}$ is the same for both alloys.

Consider now the hypothetical GB and TJ solidus lines shown in Figs. 3 and 5 by dashed and dotted lines. If the alloys are in the (Al) + L area of the bulk phase diagram, i.e. above the bulk solidus line, and σ_{GB} is higher than $2\sigma_{SL}$, the melt wets grain boundaries. In this case a GB is substituted by the layer of the liquid phase (melt) and two solid–liquid interfaces. The condition of full wetting, $\sigma_{GB} > 2\sigma_{SL}$, is fulfilled above T_{wGB}. At this temperature T_{wGB} the GB wetting tie-line exists in the two-phase area (Al) + L area of the bulk phase diagram. The wetting transition temperature, T_{wGB}, depends on GB energy, σ_{GB}. If σ_{GB} is high, T_{wGB} is low and visa versa. The minimal temperature $T_{wGB0\%}$ corresponds to the maximal GB energy σ_{GBmax}. Below $T_{wGB0\%}$ no wetted GBs (0%) are present in the polycrystal (area 1 in Fig. 3). The maximal temperature $T_{wGB100\%}$ corresponds to the minimal GB energy σ_{GBmin}. Above $T_{wGB100\%}$ all high-angle GBs in the polycrystal are wetted (area 2′ in Fig. 3). Temperature $T_{wGB100\%}$= 565 °C is taken from 4, $T_{wGB0\%} = 440$ °C was determined experimentally in [27]. Between $T_{wGB0\%}$ and $T_{wGB100\%}$ (area 2 in Fig. 3) the portion of wetted GBs in the polycrystal increases with increasing temperature. In the area 2′ above $T_{wGB100\%}$ the viscous flow of a polycrystal becomes possible even if the amount of melt is low [29,30]. Therefore, at low Zn concentrations melt lubricates the grains and they easily slide one over the other. Below

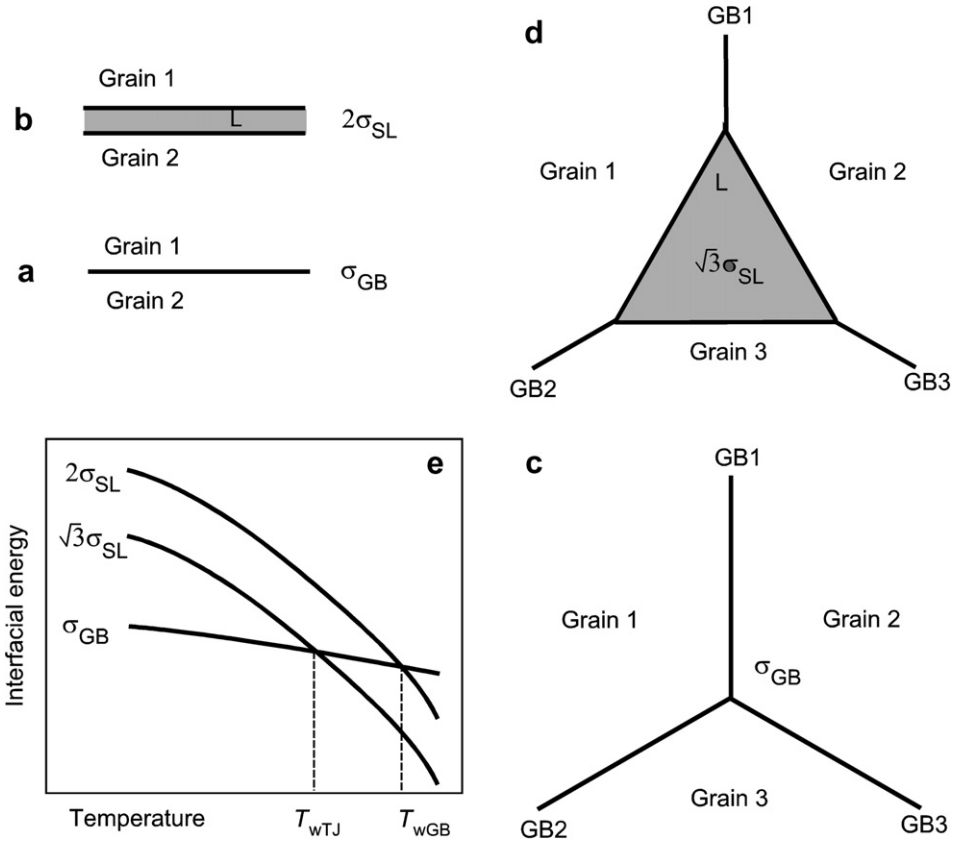

Fig. 7. (a) "Dry" grain-boundary with energy σ_{GB}. (b) Completely wetted GB, substituted by a liquid layer and two solid/liquid interphase boundaries with energy $2\sigma_{SL}$. (c) "Dry" triple junction with GBs having energy σ_{GB}. (d) GB triple junction substituted by a triangle of liquid phase. (e) Temperature dependence for GB energy σ_{GB}, energy of GB liquid layer $2\sigma_{SL}$ and energy of solid/liquid interphase boundaries surrounding the liquid triangle in the wetted triple junction $\sqrt{3}\sigma_{SL}$.

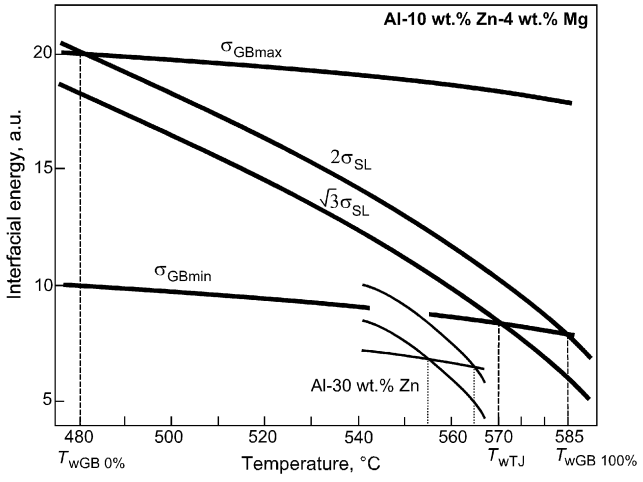

Fig. 8. Semi-quantitative scheme for the temperature dependence of interfacial energies. It illustrates the results obtained in this work.

$T_{wGB0\%}$ (the area 1) melt is enclosed in the surrounding solid phase. Therefore, at high Zn concentrations the strength of a polycrystal decreases only slightly if the solidus line is crossed from below.

If the alloys are slightly below the solidus line, i.e. in the (Al) area of the bulk phase diagram (marked as 3 in Fig. 3), a thin layer of the liquid-like phase can be formed in GBs. In this area the liquid phase can be formed in the GBs even though it is metastable in the bulk [36]. This is because the system needs the additional energy ΔG for the formation of a metastable liquid phase. This energy can be compensated if the condition of full wetting, $\sigma_{GB} > 2\sigma_{SL}$, is fulfilled and the energy gain $\sigma_{GB} - 2\sigma_{SL}$ is higher than the energy loss ΔG. In this case a thin layer of a liquid-like phase may appear in the GB. Zn concentration in the liquid-like phase is also given by the liquidus line at the respective annealing temperature.

If the alloys are deeply below the solidus line in the (Al) area of the bulk phase diagram (area 4 in Fig. 3), ΔG further increases and $\sigma_{GB} - 2\sigma_{SL}$ cannot compensate ΔG any more. The liquid-like GB layer disappears below GB solidus line (dashed line in Fig. 3). GB solidus begins at the melting point T_m of the pure component (in case of Al $T_m = 662.5$ °C). GB solidus finishes at the intersection between GB wetting tie-line and bulk solidus. Each GB with its σ_{GB} has its own wetting tie-line and respective GB solidus. Only one (hypothetic) GB solidus line corresponding to maximal GB energy σ_{GBmax} and minimal $T_{wGB0\%}$ is drawn in Fig. 3. The same is true also for the TJs. However, TJs have their own solidus line (dotted line

in Fig. 3), which is positioned below GB solidus (dashed line in Fig. 3).

The structure and composition of grain boundaries and GB triple junctions were studied by high-resolution electron microscopy and analytical transmission electron microscopy in the Al–5 at.%Zn polycrystals [31] and by differential scanning calorimetry (DSC) in the Al–7.5 at.%Zn polycrystals [37]. Between bulk solidus and GB or TJ solidus the metastable Zn-rich β_m-phase was observed in the GB triple junctions of quenched samples (open circle in Fig. 3) [31]. This phase does not appear in the samples annealed both above bulk solidus and below GB solidus. Zn-content in this β_m-phase corresponds to that of bulk liquidus. This is a structural indication that if the melt wets the GBs or TJ, the GB (or TJ) solidus line appears in the bulk phase diagram, and the liquid-like phase exists in GBs and TJs between bulk solidus and GB solidus lines (or TJ). The structural observation of this phase is also supported by the data obtained by means of DSC. Namely, the melting of the fine-grained Al–7.5 at.%Zn polycrystals starts at the temperature (full circle in Fig. 3) below the bulk solidus [37].

The presence of the thin layer of an equilibrium liquid-like phase in GBs and TJs between bulk and GB (TJ) solidus line can explain the phenomenon of unusually high plasticity of 7xxx alloys based on the Al–Zn system. Being nanograined, the 7xxx alloys possess very high elongation-to-failure ratios (up to 1250%) [29,30]. This phenomenon exists only in a narrow temperature interval, i.e. slightly below the solidus line. High superplasticity is also observable only below about 12 wt.%Zn and 5 wt.%Mg. This phenomenon remained unexplained for more than 10 years. However, it can be easily explained by the presence of GB and TJ solidus lines in the conventional bulk Al–Zn–Mg diagram (Fig. 5). It is important that these lines exist only above $T_{wGB} = 440\,^{\circ}C$, and the portion of GBs and TJs with liquid-like layers increases with increasing temperature and decreasing Mg and/or Zn concentration.

5. Conclusions

1. It follows from the simple geometric considerations that the condition for complete wetting for the grain-boundary triple junctions $\sigma_{GB} > \sqrt{3}\sigma_{SL}$ is weaker than that for the grain boundaries $\sigma_{GB} > 2\sigma_{SL}$ even if one neglects the line tension of a triple junction. It means that the $\sqrt{3}\sigma_{SL}(T)$ values are lower than $2\sigma_{SL}(T)$ at all temperatures, and the temperature of the wetting transformation for triple junctions T_{wTJ} has to be below of that for grain boundaries T_{wGB}.
2. It has been observed experimentally for the first time in the Al–30 wt.%Zn and Al–10 wt.%Zn–4 wt.%Mg alloys that this difference $T_{wGB} - T_{wTJ}$ really exists and is measurable. $T_{wGB} - T_{wTJ}$ is about 10 °C in the Al–30 wt.%Zn alloy and 15 °C in the Al–10 wt.%Zn–4 wt.%Mg alloy.

Acknowledgements

The investigations were partly supported by INTAS (contract 05-109-4951), Russian Foundation for Basic Research (contracts 05-02-16528 and 06-03-32875), and the exchange program between Russian and Polish Academies of Sciences. The authors cordially thank Prof. B.S. Bokstein, A.L. Petelin and E.I. Rabkin for stimulating discussions and Dr. A.N. Nekrasov for the help with SEM measurements.

References

[1] Cahn JW. J Chem Phys 1977;66:3667.
[2] Eustathopoulos N. Int Met Rev 1983;28:189.
[3] Straumal B, Muschik T, Gust W, Predel B. Acta Metall Mater 1992;40:939.
[4] Straumal B, Molodov D, Gust WJ. Phase Equilibria 1994;15:386.
[5] Straumal BB. Grain boundary phase transitions. Moscow: Nauka publishers; 2003 [327 p. in Russian].
[6] Islam SH, Qu X, He X. Powder Metal 2007;50:11.
[7] Wei DQ, Meng QC, Jia DC. Ceram Internat 2007;33:221.
[8] Solek KP, Kuziak RM, Karbowniczek M. Arch Metall Mater 2007;52:25.
[9] Ji ZS, Hu ML, Zheng XP. J Mater Sci Technol 2007;23:247.
[10] Shatilla YA, Loewen EP. Nucl Technol 2005;151:239.
[11] Straumal BB, Gust W. Mater Sci Forum 1996;207–209:59.
[12] Straumal B, Semenov V, Glebovsky V, Gust W. Defect Diff Forum 1997;143–147:1517.
[13] Chang LS, Rabkin E, Straumal BB, Hofmann S, Baretzky B, Gust W. Defect Diff Forum 1998;156:135.
[14] Straumal B, Gust W, Watanabe T. Mater Sci Forum 1999;294–296:411.
[15] Gottstein G, Ma Y, Shvindlerman LS. Acta Mater 2005;53:1535.
[16] Shvindlerman LS, Gottstein G. J Mater Sci 2005;40:819.
[17] McLean D. Grain boundaries in metals. Oxford: Clarendon Press; 1957. p. 95.
[18] Smith CH. Trans AIMME 1948;175:15.
[19] Pezzotti G, Nakahira A, Tajika M. J Eur Ceram Soc 2000;20:1319.
[20] Furukawa Y, Sakurai O, Shinozaki K, Mizutani N. J Ceram Soc Japan 1996;104:900.
[21] Elfwing M, Osterlund R, Olsson E. J Am Ceram Soc 2000;83:2311.
[22] Wang H, Chiang YM. J Am Ceram Soc 1998;81:89.
[23] Tanaka I, Kleebe HJ, Cinibuluk MK, Bruley J, Clarke DR, Ruhle M. J Am Ceram Soc 1998;77:911.
[24] Hier-Majumder S, Ricard Y, Bercovici D. Earth Planet Sci Lett 2006;248:735.
[25] Birol Y. Int J Mater Res 2007;98:53.
[26] Kim JH, Kim JH, Yeom JT, Lee DG, Lim SG, Park NK. J Mater Process Technol 2007;187:635.
[27] Straumal B, López G, Gust W, Mittemeijer E. In: Zehetbauer MJ, Valiev RZ, editors. Nanomaterials by severe plastic deformation. fundamentals – processing – applications. Weinheim: John Wiley, VCH; 2004. p. 642–7.
[28] Straumal BB, López G, Mittemeijer EJ, Gust W, Zhilyaev AP. Def Diff Forum 2003;216–217:307.
[29] Higashi K, Nieh TG, Mabuchi M, Wadsworth J. Scripta Metall Mater 1995;32:1079.
[30] Takayama Y, Tozawa T, Kato H. Acta Mater 1999;47:1263.
[31] Straumal BB, Mazilkin AA, Kogtenkova OA, Protasova SG, Baretzky B. Phil Mag Lett 2007;87:423.

[32] Massalski TB et al., editors. Binary alloy phase diagrams. Materials Park, OH: ASM International; 1990. p. 238–242.
[33] Dolgopolov N, Petelin A, Rakov S. Def Diff Forum 2006;249:227.
[34] Dolgopolov NA, Petelin AL, Rakov SV, Simanov AV. Isvestia VUZov Zvet Metall 2007;N2:42 [in Russian].
[35] Sutton AP, Balluffi RW. Interfaces in crystalline materials. Oxford: Clarendon Press; 1995. 807 p.
[36] Straumal BB, Baretzky B. Interf Sci 2004;12:147.
[37] Straumal B, Kogtenkova O, Protasova S, Mazilkin A, Zieba P, Czeppe T, et al. Mater Sci Eng A; 2008 (in press).